2022 Mercer Science and Engineering Fair Research Report

Modeling and Mitigating Infection Risks of COVID-19 in Aircraft Cabins

Xinkai Yu

Princeton International School of Mathematics and Science

Abstract

Taking airplanes is crucial for many people's lives, and the air distribution system plays an important role in providing a healthy environment in the aircraft cabin, especially decreasing the infection risk during the COVID-19 pandemic. This study attempted to predict, control, and manage the infection possibility in the aircraft cabin. To investigate the risk of taking airplanes with the suspected Covid-19 infectors, a model combined CFD simulation on the air distribution with the theoretical analyses on the classical Wells-Riley model was established. By developing models that are capable to simulate the air distribution inside the cabin and introducing the concept of dilution ratio, the infection risk at different locations can be estimated. In addition to the changes in the management mode, we can also consider adding some new design concepts based on the concept of "Combination of normal and epidemic". Several scenarios with different control measures were evaluated to inspect the feasibility and validity of the control of the infection rate in the aircraft cabin. The classical Wells-Riley infection model was improved and calibrated by using CFD simulation to consider the effects of social distance and ventilation effectiveness. Furthermore, good applications of the improved models were found on infection risk prediction, and this study thus provided some suggestions on pandemic controlling strategies in the aircraft cabin. This study presents an index and an improved combined model to predict and then decrease the infection possibility of respiratory transmission diseases.

Keywords: COVID-19, infection risk, control measures, CFD, improved prediction model

1. Introduction

As Covid-19 becomes a global pandemic, effectively slowing down its transmission has become a challenge worldwide. With high occupant density and long exposure time, the aircraft cabin environment is susceptible to the transmission of airborne infectious diseases [1][2]. A variety of respiratory infectious diseases, including tuberculosis [3], influenza [4], SARS [5] and norovirus transmission [6], are reported to have cross-infection during flights. Recently, there have also been cases of suspected in-flight cross-infection of Covid-19, indicating that the potential risk cannot be neglected [7].

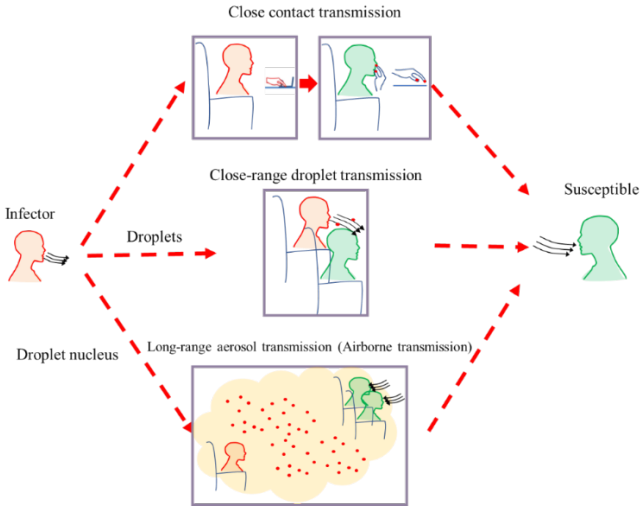

Figure 1 Three likely transmission routes of Covid-19

The pathogens of respiratory infectious diseases may be produced by sneezing, coughing, exhalation of infectors. Particles carrying these pathogens may reach the respiratory tract of susceptible persons through different routes, including 1) direct contact transmission, 2) short-range droplet transmission, and 3) long-distance, aerosol (or airborne) transmission [8]. For the first two, the transmissions are limited to the close range of the infector. The aerosol transmission, on the other hand, can reach much longer distances together with the airflow. Hence, evaluating the aerosol transmission of the COVID-19 in the aircraft cabin is essential for the reduction of the aircraft cabin infection risk.

Quantitative infection risk models are essential tools for understanding risks and evaluating the effectiveness of infection control measures. A quantitative infection risk model that can accurately predict the airflow and aerosol dispersion in the aircraft cabin is critical to assess the risk of airborne transmission of COVID-19. Risk assessment usually uses a probabilistic

method to quantitatively describe the possibility of an individual or a population of infectious diseases based on theories and mathematical equations, which are biologically reasonable and in line with clinical or laboratory evidence. The Wells-Riley equation is one of the classic aerosol-borne infection probability models. In 1974, Riley et al. proposed the equation to describe the spread of infectious disease and achieved remarkable success in explaining a measles outbreak [9]. ASHRAE report recommended using the Wells-Riley equation to describe the aerosol transmission of the new coronavirus [10]. It has been proved that certain factors (especially ventilation rate) influence aerosol transmission [11].

Due to the high density of occupancy in the cabin, the airflow field in the aircraft cabin is non-uniform, influenced by both the forced convection due to mechanical ventilation and natural convection due to human buoyance. Figure 2 shows the flow field characteristics of the aircraft cabin section [12]. This special flow can form two vortex areas near the passengers. The upper supply diffuser causes downwards flow in the corridor, and the buoyance effect generates upward flow near the passengers. The entire cabin forms a "saddle"-shaped flow field distribution.

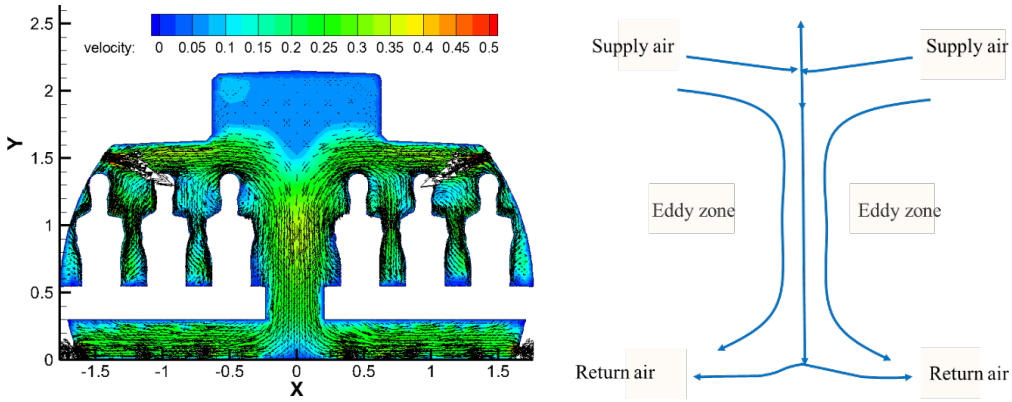

Figure 2 Illustration of flow field characteristics of aircraft cabin

The aircraft flow field can be further divided into zones. The flow in the zone around the human body is dominated by the thermal plume of the human body, forming an upward airflow. This zone is designated as the "thermal plume dominant zone". The airflow at other locations is mainly affected by supply air jets and return air location, forming the "main air supply area".

However, the classic Wells-Riley equation is only suitable for risk assessment in a uniform and steady-state environment, and cannot be directly used in a dynamic non-uniform distribution scenario such as an aircraft cabin. A risk assessment model in a non-uniform environment that

combines the aircraft's inhomogeneous field characteristics with the classic Wells-Riley infection risk assessment method is essential. Therefore, it is important to simulate the flow and particle concentration field characteristics accurately. Meanwhile, it is also necessary to establish a method for calculating the infection risk based on the concentration field of virus-laden particles.

This study developed an improved model based on the traditional Wells-Riley equation. Improvement was made by introducing the local dilution factor distributions for given pollutant release sources and ventilation conditions. Based on the risk assessment model, the infection risks inside the aircraft cabin under different modification measures were analyzed. A quick semi-empirical model has also been established for the quick evaluation of the infection risk in the aircraft cabin.

2. Methods

2.1 Classic model for predicting the infection risk

According to the Wells-Riley model, the infection risk of an aerosol-borne disease in a well-mixed stable environment can be estimated by [9]

$$P = \frac{C}{S} = (1 - e^{-Iqpt/Q}) \quad (1)$$

where P is the infection risk; C is the number of cases that develop infection; S is the number of susceptible people; I is the number of source patients (infectors); q is the quanta generation rate produced by one infector (h^{-1}); p is the pulmonary ventilation rate of each susceptible person (m^3/h); t is the exposure time (h); Q is the total ventilation (virus-free) flow rate (m^3/h). The quanta generation rate (q) is the most important parameter in the model. 1 quantum is defined as a collection of pathogen particles that can infect a susceptible individual. Assuming that the susceptible object will be infected after inhaling N parts of pathogen particles, the N parts of pathogen particles can be "packaged" and called 1 quantum. The number of pathogen particles in a quantum is uncertain, which is related to the specific disease. Therefore, quantum is similar to the release source intensity of droplet nuclei but is different from the release source intensity of a continuous gas source. It can be considered that the emitted quanta are discrete.

2.2 New model (A) - considering dilution ratio

When the environment is complex and there is an uneven spatial distribution of pathogen particles, the classical Wells-Riley equation is no longer directly applicable. A model based on the traditional Wells-Riley equation was improved by introducing the local dilution factor distributions for given pollutant release sources and ventilation conditions.

A new parameter, the local dilution ratio, is thus proposed. The dilution ratio (Dr) is the "concentration" of quanta at the location of the susceptible person divided by the "concentration" of quanta in the breath of the infected person. Therefore, it is a dimensionless parameter. In addition, the dilution ratio can vary from location to location, making it possess the property of the "field". This parameter is proposed by our research team and is used in the prediction of aircraft environments for the first time.

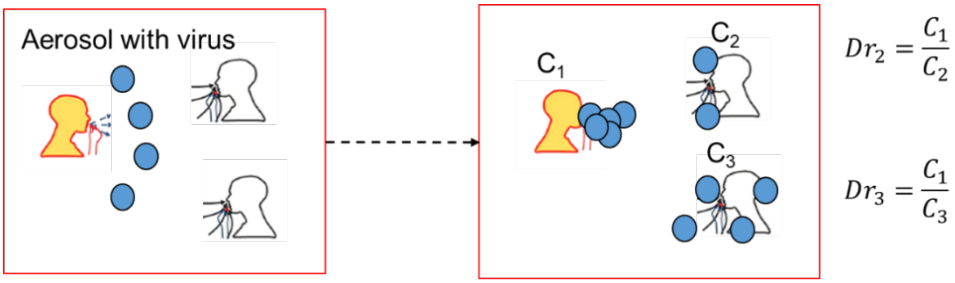

Figure 3 Schematic diagram of the distribution of virus particles exhaled by an infector in the aircraft cabin and illustration of the concept dilution ratio (Dr).

Since the "concentration" of quanta contained in the breath of an infector is the generation rate of quanta divided by the volume of respiration, the expected quantum pathogen per unit volume at the point where a susceptible person is located in:

$$E = \frac{E_0(1-\eta_I)}{Dr} = \frac{q(1-\eta_I)}{pDr} \quad (2)$$

Where E is the quanta concentration (quanta/m^3) at the location of the susceptible person; E_0 is the quanta concentration in the breath of the infector (quanta/m^3); Dr is the local dilution ratio, and q is a quanta generation rate of the infector (quanta/h); p is the respiratory ventilation of the susceptible person (m^3/h), and η_I is the particle filtration efficiency of the mask to the exhaled breath of the infector.

It can be seen that the expected number of inhalation per unit time is q (1-η_I)/Dr. Therefore, local infection risk based on the dilution ratio can be obtained as follows:

$$P_{local} = (1 - e^{-qt(1-\eta_I)(1-\eta_s)(p_s/p_I)/Dr}) \quad (3)$$

Where P is the estimated infection rate at a local position; q is the quanta generation rate of an infector (quanta/h); t is the exposure time (h); Dr is the dilution ratio; η_I and η_s are the mask filtration efficiency of the infector and susceptible person, respectively; p_I and p_s are the respiratory rate of the infector and susceptible person respectively, which are considered the same in most cases.

The introduction of the dilution ratio makes it easier to analyze the risk in a complex and non-uniform environment in combination with the CFD simulation. Taking the breath of the infector as the particle source, the dilution ratio of the exhaled breath of the infector at the location of the susceptible person can be calculated by CFD, to further estimate the infection risk.

$$Dr = \frac{\text{The concentration ininfector's exhalation}}{\text{The concentration in susceptible's exhalation}} \quad (4)$$

2.3 CFD simulation method

CFD (computational fluid dynamics) model has been widely used in simulating the flow, temperature, and pollutant distribution in aircraft cabins [14]. A commercial CFD program, FLUENT (Fluent, 2005), was used. The particle phase is regarded as a continuous phase to solve the conservation equation of particles. There are two widely used Eulerian methods: multiphase flow model and drift flux model.

A complete aircraft cabin often has dozens of rows of seats, simulating the entire cabin would be extremely time-consuming and expensive. Liu et al. [15] and other studies suggested that for the purpose of understanding the detailed effect of ventilation and microenvironment around a person (infector) and surrounding passengers (susceptible), simulating a section of the cabin would not lose insight for this particular purpose. The reasonable number of rows in the passenger cabin is suggested to be five, preferably seven. Hence, we adopted a section of seven rows for detailed simulations. The tetrahedral grid was adopted in this study. The grid number of the 7-row cabin simulated in this study reached at least 9 million.

2.3.1 The boundary condition of the aircraft cabin

An accurate boundary condition of temperature is essential for flow field simulation. The

human body surface temperature mainly comes from the literature [18] [19]. At this temperature, the human body can produce a thermal plume similar to the actual situation. Other boundary conditions come from the research of Li and others on the simulation of pollutants in the aircraft cabin [17]. The infector was assumed to be at the middle seat of the fourth row. The exposure time was 2 hours and the quanta generation rate from the infector was 20 quanta/h. The air supply volume was set according to the value of Airworthiness Standards, and the corresponding ventilation volume was 8L/s/p. Facial masks are the simplest and easy-to-implement personal protection device in the cabin so it is considered in the study. There are uncertainties about the particle filtration efficiency of different types of masks. Masks of the same specification from different manufacturers could also have differences in filtration efficiency. The efficiency of the surgical mask was 33.3% [20].

3. Results and discussion

3.1 Characteristics of the flow field

The whole field was planned and marked with the axis shown in Figure 6. The lateral directions were marked with the X-axis. The up and down were marked with the Y-axis. And the anterior and posterior directions were marked with the Z-axis (Figure 4a). In addition, different positions can be further numbered. Each column was 1 to 7, and the lateral direction was a to f (as shown in Figure 4b). Two locations of Z = 3.1 m and Z = 3.5 m were intercepted for further flow-field analysis.

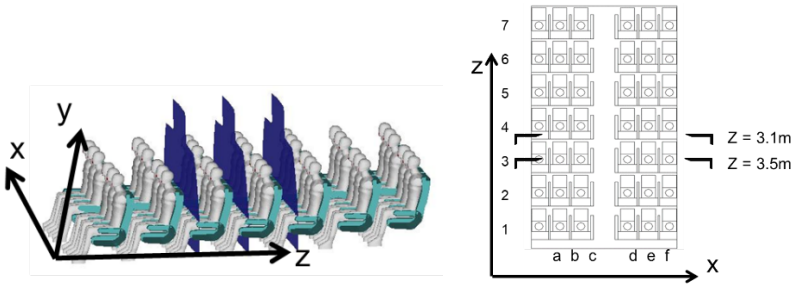

a) Axis identification b) Seat identification

Figure 4 Identification method of the aircraft cabin

It can be observed that the whole air supply forms a "saddle"-shaped flow field distribution in the aircraft cabin, as shown in Figures 5, which was the "main air supply area". The "thermal

plume dominant area" could also be observed, which was circled by the red dotted line in Figure 5. The airflow around the human body was affected by the human thermal plume and moved upward along the human body. When it reached the head position, it was suppressed by the horizontal air supply and could not continue to flow upward, resulting in an area named "thermal plume dominant zone". The characteristics of the whole flow field were similar to those in the literature [12].

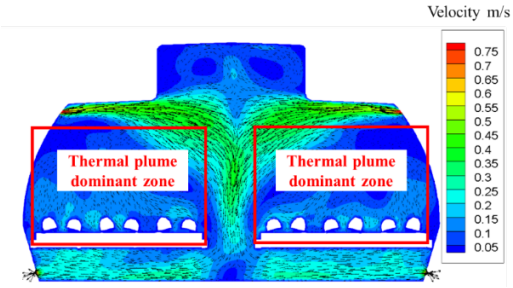

Figure 5. Flow field characteristics at cross-section Z=3.5

3.2 Characteristics of dilution ratio

Figure 6 shows the distribution of dilution ratio (Dr) at the same plane. The dilution ratio has been increased to 5000 at two rows away from the infector. The passenger next to the 4-b infector at the aisle side had the greatest impact. The main reason was that the special "saddle"-shaped flow field led to the droplet nuclei from the infector in the middle sucked to the aisle side passenger. The transmission of virus particles seems to be limited to the front and back row around the infector. Such a zoning effect would be beneficial to control the widespread infection inside the cabin.

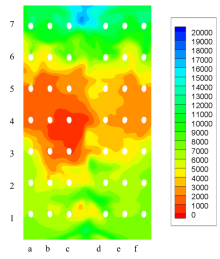

Figure 6. Distribution of dilution ratio (Dr) at Y = 1.2m

3.3 Distribution characteristics of infection risk

The infection risk of passengers in different locations was further analyzed. A breathing zone

was defined for each passenger, and the average concentration or dilution ratio in the breathing area was used to assess the risk of infection of the passenger. Figures 7 show the distribution of infection rate at the height of Y = 1.2m and the breaths zones. By observing the infection rate distribution, it is regional and non-uniform. The infection rate was relatively high around the infector and decreased significantly with the distance. If we set 1% as the “tolerable infection risk”, the impact would be limited to 4-a, 4-b, 4-c, 5-a, 5-b, and 3-c. The risks were much lower outside this zone. The results again indicated that the zoning effect was achieved and special attention should be paid to regions to close proximity of the infector.

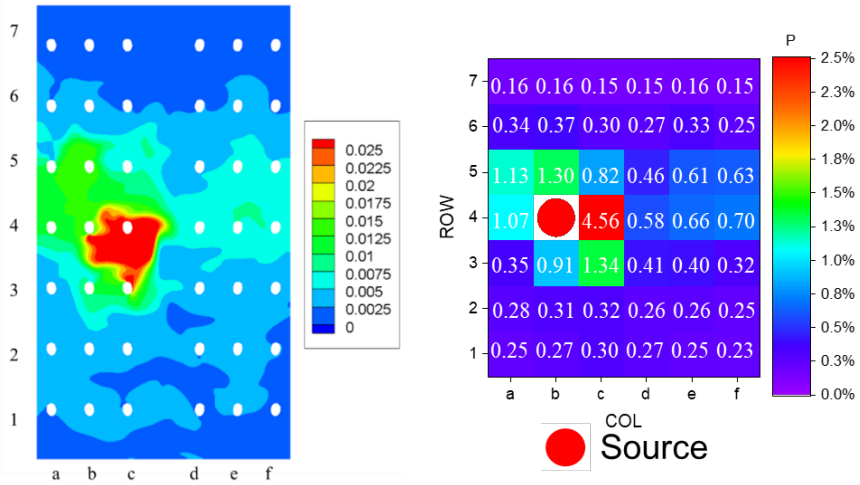

(a) 1.2m (b)breath zones

Figure 7. Distribution of infection rate at Y = 1.2m and breathe zones

3.4 Controlling COVID-19 transmission in Different schemes

Based on the concept of "combination of normal and epidemic conditions", propose the method of improving the whole airflow design and micro air distribution of the breathing area to reduce the transmission risks while not posing major changes to the current ventilation system and ventilation rate. In addition to the changes in the management mode, we can also consider adding some new design concepts based on the concept of “Combination of normal and epidemic”. The schemes were used to strengthen the zoning effect in the aircraft cabin and prevent changing the flow model of the aircraft cabin. The flow field could be abstracted as the following figure, all the schemes should be careful to change the flow mode.

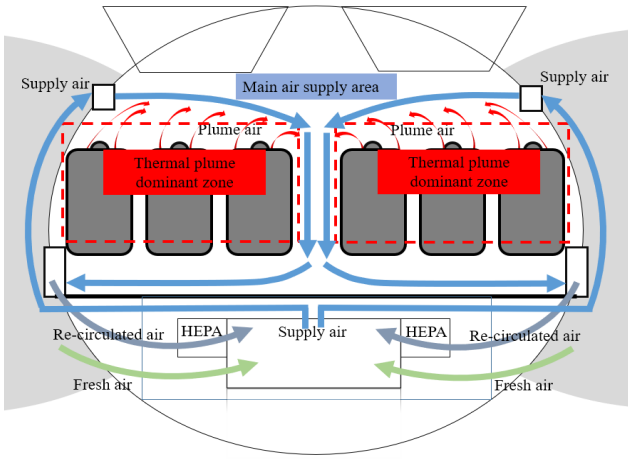

Figure 8. Characteristics of the "saddle"-shaped flow field

3.4.1 Retractable isolation baffle between passengers

The retractable isolation baffle between passengers to reduce the risk of infection in the cabin during the epidemic period was proposed. From the research above, the cross-transmission risk between the seats in the same row is relatively high. Therefore, the design of the isolation baffle is mainly to isolate the virus particles of this part, to reduce the infection risk between the left and right adjacent seats. Specifically, the isolation baffle mainly increases the left and right physical separation, to increase the actual social distance between passengers, as shown in Figure 9. Next, we will further study and discuss the effect of adding isolation baffle and the influence of the baffle height. Scenario I (the height of the isolation baffle exceeds the top of the passenger's head) and Scenario II (the height of the isolation baffle reaches the mouth of the passenger) are designed for the study.

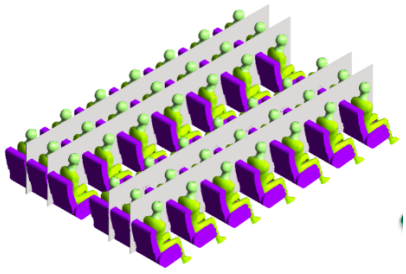

Figure 9. Schematic diagram of using isolation baffle between passengers

There is no obvious influence on the horseshoe shape of the mainstream, but the rising thermal plumes of the passenger are separated by the baffles, as shown in Figure 10. This may reduce

the impact between the same row and same column. However, the cross-flow of different rows has been strengthened.

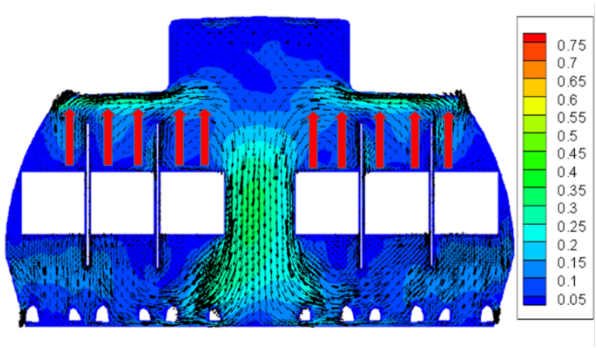

Figure 10. The airflow field of Scenario I

The infection risk distribution of Scenario I in the cabin is shown in Figure 11. Due to the barrier of the isolation baffle, the virus-laden particles emitted from the infection source at 4-b can only pass over the upper part of the baffle, which reduces the risk of infection of the passengers at 4-c. The comparison of infection risk between Scenario I and Basic Case is shown in Figure 12. From the figure, we can see that the overall risk of infection has been significantly reduced, the highest infection rate is only 2.7% and 41% lower than that of the Basic Case. The improvement effect is equivalent to Scenario B (reduce the number of passengers by 1/3) as shown in follows.

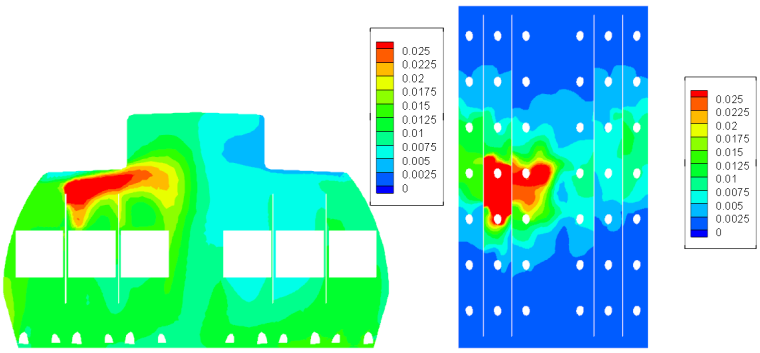

a) z = 3.3 m b) y = 1.2 m

Figure 11 The infection risk distribution of Scenario I

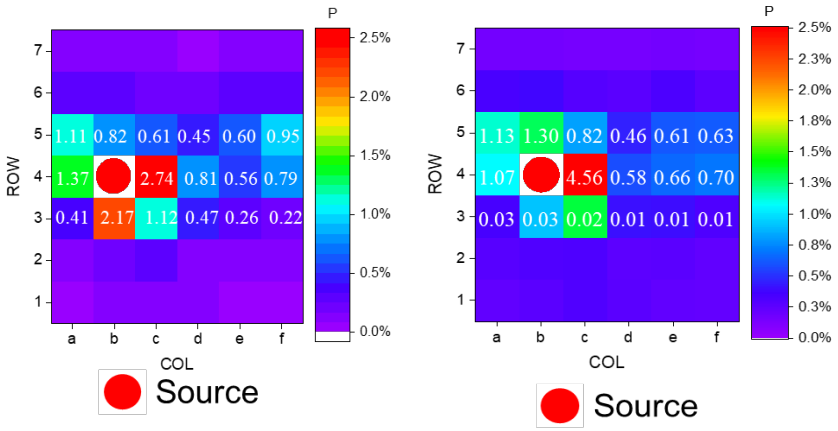

a) Scenario I b) Basic Case

Figure 12 Comparison of infection risk between Scenario I and Basic Case

3.4.1.1 Influence of the height of isolation baffle

The above studies prove that the isolation baffle can effectively reduce the risk of infection when the height of the isolation baffle exceeds the top of the passenger's head (Scenario I). Next, we will analyze the influence of the height of the isolation baffle. Scenario II when the height of the isolation baffle reaches the mouth of the passenger is analyzed.

The comparison of infection risk between Scenario II and Basic Case is shown in Figure 13. It is found that the highest infection risk of Scenario II was even higher than that of Basic Case. This is because the thermal plume must flow away from the upper part of the human body, and the thermal plume reaching the mouth will help the virus-laden particles to reach the breathing area of the nearby passengers. The results show that in order to achieve e better isolation effect, the height of the isolation baffle should exceed the top of the passenger's head.

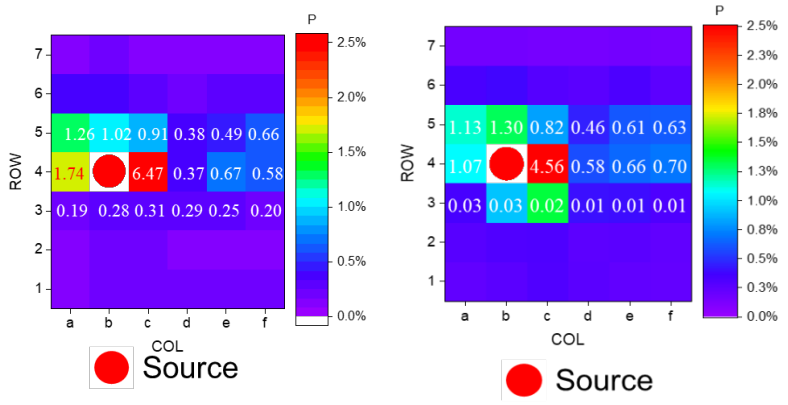

a) Scenario II b) Basic Case

Figure 13 Comparison of infection risk between Scenario II and Basic Case

3.4.2 A filtration on the isolation baffles

Cross infection risk between the same row seats is relatively high. Adding "retractable isolation baffles" between adjacent seats and filtrations on the isolation baffles. Figure 14 shows the change of the baffles and the filtrations.

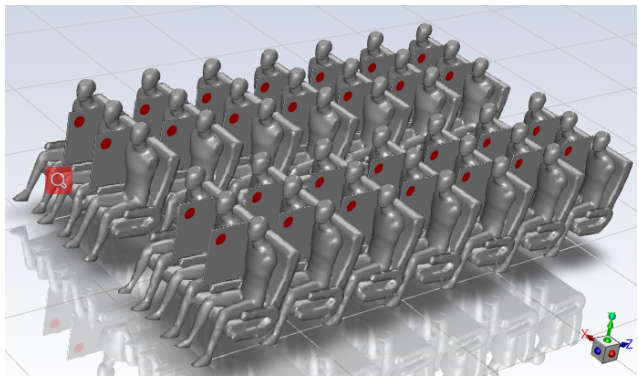

Figure 14 Schematic diagram of using isolation baffles with filtrations between passengers

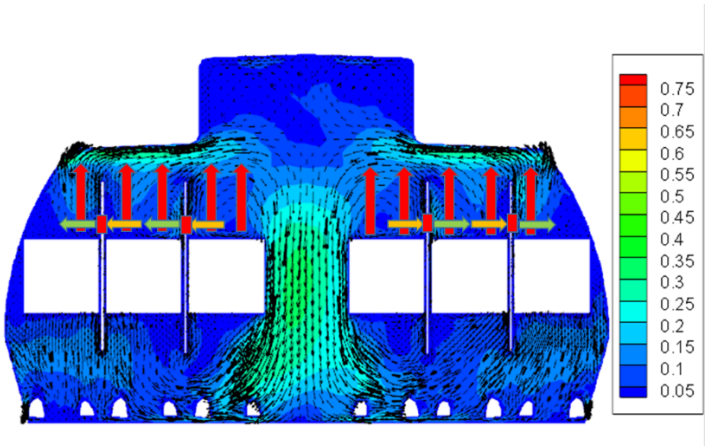

Figure 15. The flow field of the filtration case

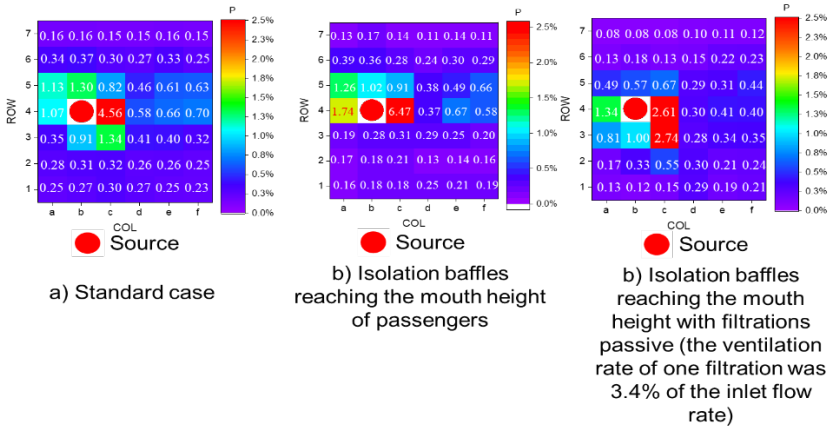

Figure 16 Comparison of infection risk between Standard case, isolation baffles, and isolation

baffles with filtrations.

Figure 16 shows the comparison of infection rates of the standard case, isolation baffles, and isolation baffles with filtrations. The infection rates of isolation baffles with filtrations were better than that without the filter, which might be caused by the flow field in the aircraft cabin is mainly along with left-right seats and the flow in different rows was hardly mixed. Therefore, the added filter can well reduce the aerosol along the same row. However, it was still noted that the mix of different rows caused by the use of isolation baffles still existed, but the addition of filters has limited the effect on the problem.

3.4.3 Add the motive outlet on the back of the seats.

Adding “retractable isolation baffles” between adjacent seats and filtrations on the isolation baffles. Figure 17 shows the motive outlet on the back of the seats.

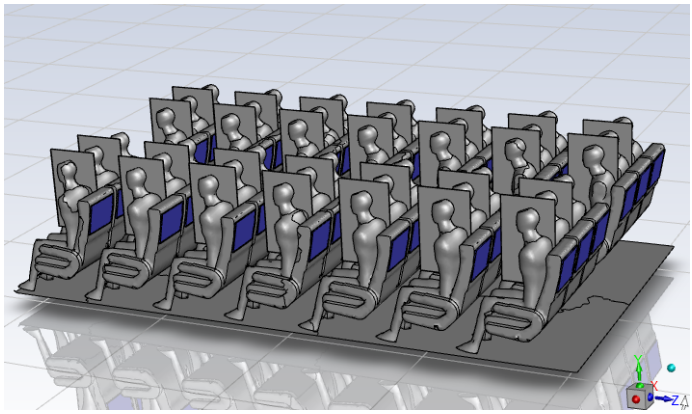

Figure 17 Schematic diagram of using isolation baffles and motive outlets on the back of the seats between passengers

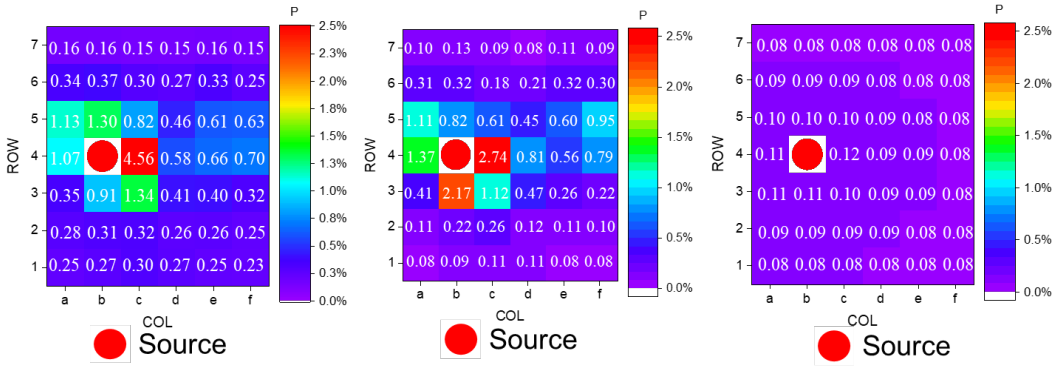

a) Standard case

b) Isolation baffles baffle over the head of passengers

c) Outlet on seats (60% flow out from seat outlets)

Figure 18 Comparison of infection risk

The return air behind the seat is added was much better than just using the isolation baffles. Using the return air behind the seat limited the spread of the particles exhaled and the return air from the front seat reduces the mix of a row. However, the use of this scheme needed a large-scale transformation of the whole aircraft cabin structure. This method was only beneficial to reduce the infection rate.

3.4.4 Whether the gaspers could be used or not

When flying under pandemic, whether the gaspers could be used or not. This is not only related to the overall airflow in the cabin but also related to the locations of the infector and other healthy people. This was unaware or even overlooked because people tend to only consider the general airflow from the ventilation and the buoyancy flow from the passengers.

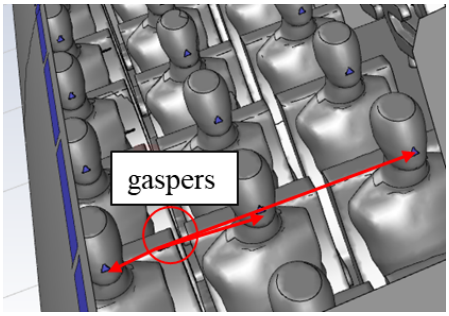

Figure 21 Schematic diagram of using the gaspers

Whether gasper is used or not, the influence on the flow field is obvious. When a gasper is used, the zoning in the whole flow field is affected to a certain extent. As shown in the figure below. Therefore, it can be said that the use of gasper is not conducive to reducing the transmission of infection rate. As the zoning effect of the aircraft, the cabin has been destroyed.

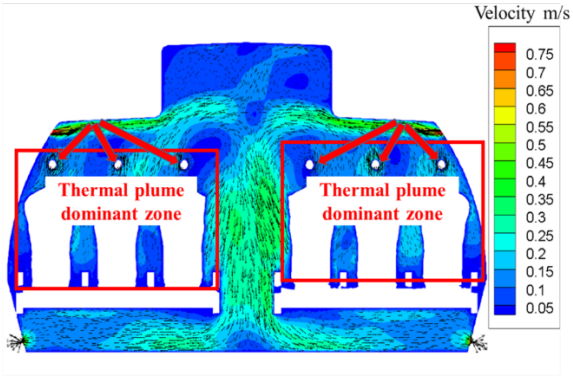

Figure 22. The flow field of the filtration case

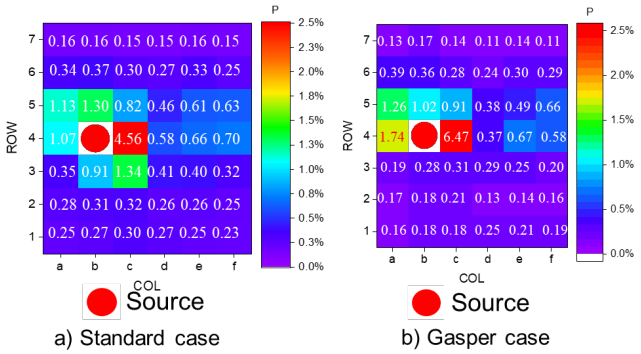

Figure 23 Comparison of infection risk between Standard case and gasper case.

3.4.5 Discussion of the schemes

It is necessary to review the characteristics of the flow field in the cabin: less front and rear crossflow and more left and right crossflow. The characteristics of the flow field can significantly reduce the spread of infectious diseases. For all improvement measures, it is best not to destroy the characteristics of this flow field. Reviewing the flow fields of the above schemes, the diaphragms in scheme 1, scheme 2, and scheme 3 obstruct the left and right flow of the flow field to a certain extent. Therefore, a new scheme to get better results without changing the flow field was designed. First of all, we know that there is a thermal plume in the aircraft, so we install an exhaust device on the ceiling to let the air return from the ceiling, so as to make the direction of the thermal plume consistent with the return direction to reduce the infection rate. A new scheme using a ‘hat outlet’ of "combination of normal and epidemic conditions" was designed and the infection rate was reduced by the new scheme.

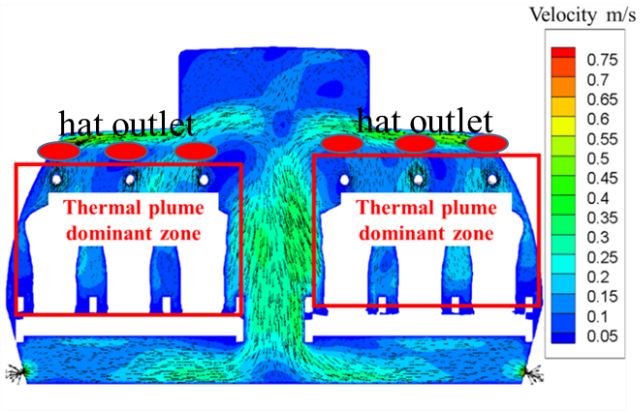

Figure 24 Schematic diagram of ‘hat outlet’ of "combination of normal and epidemic

conditions"

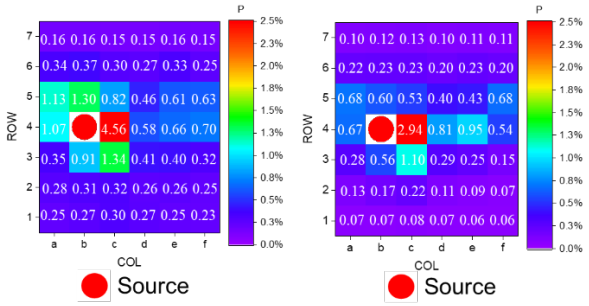

a) Standard case b) with hat outlet

Figure 25 The infection rates of the 'hat outlet'

3.5 New model (B) -considering the social distance and ventilation effectiveness

Although the new model considering dilution ratio combining the CFD simulation was established, the calculation time of one case was still at the hour level. For rapid calculation of the infection risk, the classic Wells-Riley model has been modified by Sun et al [13]. However, how to obtain the parameters of the model was still a scientific problem. For better management of the aircraft cabin, a new method to fit the parameters of Sun's model was established and validated.

3.5.1 Sun's model and the parameters [13]

The relationship between the statistical probability of droplets in different sizes and their transmission distances was built based on the analysis of distribution and transmission of the experimental exhaled droplets. The social distance index Pd (%) is expressed as a function of distance d (m), where Pd is a cumulative percentage or probability and its upper limit is 100 %. Principally, Pd increases with the decrease of transmission distance that is negatively related to droplet size. The equation of the Pd was shown as follows:

$$Pd = (-18.19\ln(d)+43.276)/100 \quad (5)$$

For a confined space or zone, different ventilation systems or modes may bring different air distribution patterns and thus efficiencies. Among all of the air distribution configurations, ceiling supply of cool air and ceiling supply of warm air with floor return are often taken as the

base cases for air distribution evaluation, respectively, with assignment 1.0 of ventilation factor in ASHRAE 62.1 (ASHRAE, 2019). This value is called air distribution effectiveness Ez and it ranges from 0.5, where makeup supply outlet is located less than half the length of the space from the exhaust, return, or both, to 1.5 with stratified air distribution systems or personalized ventilation system, as summarized in Table 1. In the outbreak of respiratory diseases such as COVID-19, this ventilation factor is particularly important for the assessment of effective ventilation in confined spaces. Computational fluid dynamics (CFD) techniques can be used to simulate individual cases and obtain more accurate and case-specific Ez.

Two important indices described above, Pd and Ez, were thus introduced into the Wells-Riley model, as presented in Eq. (6).

$$P = \frac{C}{S} = (1 - e^{-f(P_d) Iqpt / QE_z}) \quad (6)$$

The study firstly attempted to calibrate the q value in the model by using one real pandemic case with other known parameters and then verified this modified model with other existing cases. The study then applied this modified model to predict the infection risk of COVID-19 in a variety of confined scenarios with different occupation densities and to investigate the required minimum ventilation rate for these spaces to achieve the targeted 2% infection probability.

3.5.2 The method to obtain the parameters

The New model (A) established in section 2.2 can calculate the infection rate of different positions, especially different passengers, in the aircraft cabin. Using the simulation results shown in section 3.3, the relationship between distances and probability could be obtained in the aircraft cabin for different passengers (Figure 22). As the distance between the source and susceptible passengers turned longer, the infection rates turned lower. Furthermore, the relationship between PI and PD can be calculated according to equation 5, so as to obtain the relationship between f (PD) and PD in equation 5.

Figure 23 shows the relationship between f(PD) and PD, from which it can be seen that the relationship between f(PD) and PD is basically linear. Using the linear test method, the linearity

of this function can be obtained as R = 0.4 and the significance is not equal to 0. Therefore, a linear fitting curve can be obtained by fitting the results. The formula is as follows: f(PD) = 1.21*Pd - 0.278. However, it should be noted that f(PD) should be greater than 0. So real f(PD)(P_I) can be written as follows:

$$\begin{aligned} P_I &= 1\text{- exp }(-(\ 1.21Pd\text{-}0.278\ )\ *\ Iqpt/Q) \qquad PD > 0.23 \\ &= 0 \qquad\qquad\qquad\qquad\qquad\qquad\qquad\qquad\qquad\qquad PD<=0.23 \end{aligned} \tag{7}$$

With equation 5 for the Pd, the infection risk of an aircraft cabin could be evaluated quickly.

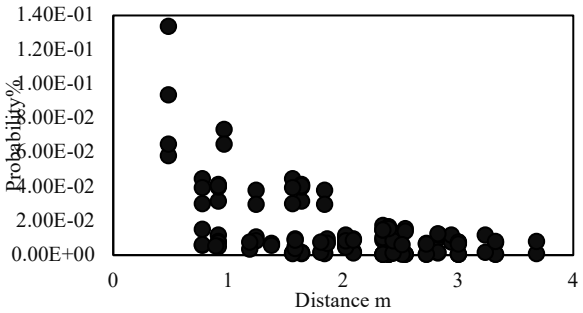

Figure 26. The relationship between the distance and probability

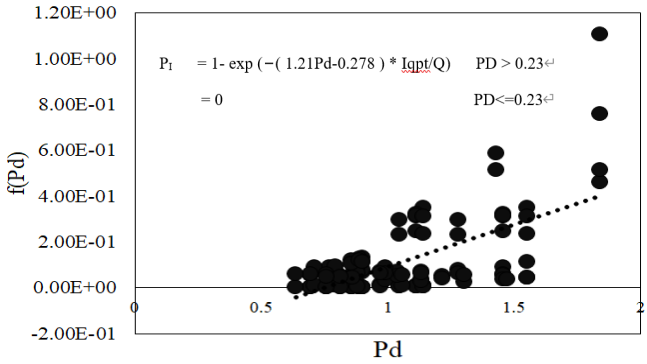

Figure 27. The relationship between f(PD) and PD

3.5.3 Influence factors

In this section, the difference of influence factors, including different ventilation, exposure time, and quanta generation rate has been evaluated. Equations 5 and 7 were used in this section.

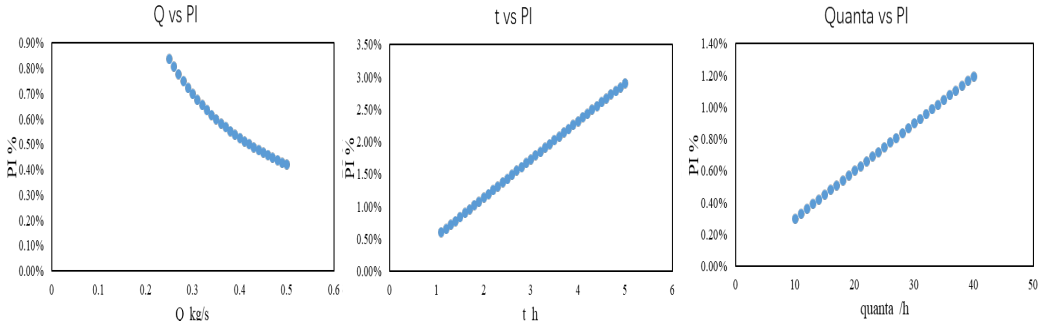

Figure 28. Change the influence factors for the model

With the increase of ventilation rates, it can be found that the infection rate is decreasing. With the increase of exposure time and quanta generation rate, it can be seen that the infection rate is increasing. This is completely consistent with the effect of CFD simulation results on the infection rate, but the simulation time is from nearly 1 hour to basically immediately, which greatly saves the estimation time for the aircraft manager.

3.5.4 Validation

The results can be verified through another CFD case. The following figure shows the comparison between CFD simulation results and model calculation results when the ventilation is 1.2 times. From the results, it can be seen that the results calculated by our fast calculation model are significantly consistent with those obtained by actual CFD calculation and simulation. Therefore, it also proves that the model is accurate and reliable, and can be effectively used to quickly calculate the infection rate at different locations.

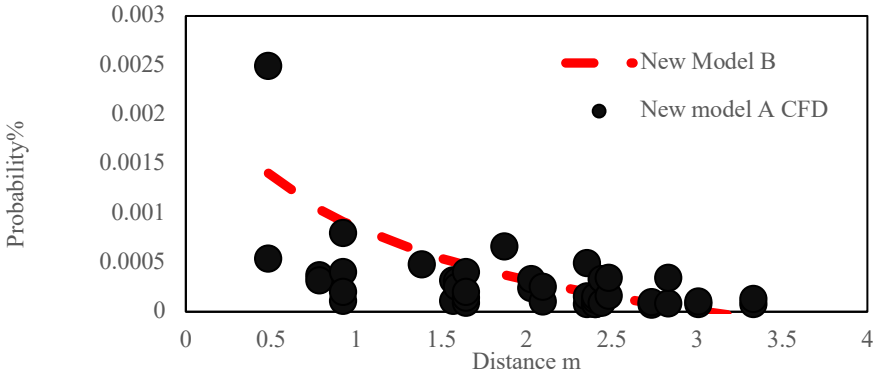

Figure 29. The validation of the model.

4. Conclusion

In this project, the airfields inside are treated as non-uniform which is closer to reality. To deal with this situation, the COVID-19 risk assessment model has been established. Based on the actual parameters in the aircraft cabin and the infector, the model provides simulations of the flow field and concentration field inside the aircraft cabin. Combining with the new concept, dilution ratio, we are able to apply the modified Wells-Riley equation to different locations within the cabin, and the infection risk can therefore be estimated.

The infection risk distribution indicated that the influence of the infection source was limited between the front and rear rows of the infector, mainly affecting the passengers on the same side. This project also found an important “zoning effect” around the infector, whereby special attention could be paid to limit locations instead of the entire cabin. The finding of this zoning effect is of great significance for the prevention and control of airborne transmission in the aircraft cabin.

Based on the concept of “Combination of normal and epidemic”, different schemes have also been designed and evaluated based on the flow field of the aircraft cabin and the “zoning effect”. The retractable isolation baffle between passengers is proposed to reduce the risk of infection in the cabin during the epidemic period. However, the setting of the height of the isolation baffle should be more careful about the reduction of the infection risk. Filtration on the isolation baffles and adding a motive outlet could strengthen the reduction of the infection risk. Furthermore, as an adverse example, the gasper had an adverse effect on the control of the infection risk. The “hat outlet” could also reduce the infection risk as it is appropriate to the flow field of the aircraft cabin.

A rapid and simple method to predict the infection rate in aircraft cabins according to distances was established. This method considers the distance of the virus transmission and uses the data of the simulated aircraft cabin to fit the parameters. This method can shorten the calculation time from the hour level to the second level and can reflect the different distances and positions.

References

[1] Houk, V.N., Baker, J.H., Sorensen, K. and Dent, D.C. (1968) The epidemiology of tuberculosis infection in a closed environment, Arch. Environ. Health, 16, 26–50.

[2] Mangili, A. and Gendreau, M.A. 2005, Transmission of infectious disease during commercial air travel, *Lancet*, 365, 989–996.

[3] Kenyon, T.A., Valway, S.E., Ihle, W.W., Onorato, I.M. and Castro, K.G. (1996) Transmission of multidrug resistant mycobacterium tuberculosis during a long airplane flight, *N. Engl. J. Med.*, 334, 933–938.

[4] Moser, M.R., Bender, T.R., Margolis, H.S., Noble, G.R., Kendal, A.P. and Ritter, D.G. (1979) An outbreak of influenza aboard a commercial airliner, *Am. J. Epidemiol.*, 110, 1–6.

[5] Olsen, S.J., Chang, H.L., Cheung, T.Y., Tang, A.F., Fisk, T.L., Ooi, S.P., Kuo, H.W., Jiang, D.D., Chen, K.T., Lando, J., Hsu, K.H., Chen, T.J. and Dowell, S.F. (2003) Transmission of the severe acute respiratory syndrome on aircraft, *N. Engl. J. Med.*, 349, 2416– 2422.

[6] Kirking, H.L., Cortes, J., Sherry, B., Hall, A.J., Cohen, N.J., Lipman, H., Kim, C., Daly, E

[7] Jianyun, L., G. Jieni, and L. Kuibiao. (2020) COVID-19 Outbreak Associated with Air Conditioning in Restaurant, Guangzhou, China. *Emerg. Infect. Dis.* 26.7.

[8] Tellier R, Li Y, Cowling B J, et al. Recognition of aerosol transmission of infectious agents: a commentary. *BMC Infectious Diseases* 2019, 19(1): 101.

[9] Riley E C, Murphy G, Riley R L. Airborne spread of measles in a suburban elementary school. *American Journal of Epidemiology* 1978, 107(5): 421-432.

[10] Schoen L J, Hodgson M J, McCoy W F, et al. ASHRAE position document on airborne infectious diseases. ASHRAE: Atlanta, GA, USA. 2020-04-29.

[11] Escombe AR, Oeser CC, Gilman RH, Navincopa M, Ticona E, et al. Natural ventilation for the prevention of airborne contagion. *PLoS Medicine* 2007, 4: e68.

[12] Yang Caiqing, 2016. Study on the distribution and diffusion characteristics of environmental pollutants in aircraft cockpit (postdoctoral report, Tsinghua University).

[13] Sun C, Zhai J Z. The Efficacy of Social Distance and Ventilation Effectiveness in

Preventing COVID-19 Transmission[J]. Sustainable Cities and Society, 2020, 62:102390

[14] Chen Q, Ventilation performance prediction for buildings: A method overview and recent applications. *Building and Environment* 2009,44(4), 848-858.

[15] Liu Sumei, 2012. Numerical Simulation of Reasonable Row Number and Pollutant Dispersion in Passenger Cabin (Master's Thesis, Tianjin University, China).

[16] Liu W, Wen J, Lin CH, Liu J, Long Z, Chen Q, Evaluation of various categories of turbulence models for predicting air distribution in an airliner cabin. *Building and Environment* 2013, 65: 118-131.

[17] Yu G, Yu B, Sun S, and Tao W Q, Comparative study on triangular and quadrilateral meshes by a finite-volume method with a central difference scheme. *Numerical Heat Transfer B-Fundamentals* 2012, 62(4):243-263.

[18] Li M, Zhao B, Tu J, et al. Study on the carbon dioxide lockup phenomenon in aircraft cabin by computational fluid dynamics. *Building Simulation*. 2015, 8(4): 431-441.

[19] Gao N, Niu J. CFD study on micro-environment around human body and personalized ventilation. *Building and Environment*, 2004, 39(7): 795-805.

[20] Bowen L E. Does that face mask really protect you? *Applied biosafety*, 2010, 15(2): 67-71.